^{18}F-Fluoroerythronitroimidazole Radiation Dosimetry in Cancer Studies

Tuula Tolvanen, MSc[1]; Kaisa Lehtiö, MD[1]; Jarmo Kulmala, PhD[2]; Vesa Oikonen, MSc[1]; Olli Eskola, MSc[3]; Jörgen Bergman, MSc[3]; and Heikki Minn, MD[1]

[1]Turku PET Centre, Turku University Central Hospital, Turku, Finland; [2]Department of Oncology and Radiotherapy, Turku University Central Hospital, Turku, Finland; and [3]Radiopharmaceutical Chemistry Laboratory, Turku PET Centre, Turku, Finland

^{18}F-Fluoroerythronitromidazole (FETNIM) is a new promising PET tracer for imaging tumor hypoxia. Accurate radiation dosimetry is important for estimating absorbed radiation doses to patients and for calculating the allowable injected dose. **Methods:** Radiation absorbed doses were estimated from PET scans obtained on cancer patients on the basis of the MIRD procedure. Dynamic acquisition data was obtained from the thorax, abdomen, and head and neck regions. The tracer was injected intravenously and mean injected activity was 366 MBq (range, 288–385 MBq). Arterial blood was continuously assayed over dynamic PET imaging. The bladder wall dose was evaluated from the voided urine activity measurements. **Results:** The effective dose to a 70-kg adult was 0.015 or 0.019 mSv/MBq, calculated on 2- or 4-h voiding intervals, respectively. The critical organ proved to be the urinary bladder wall, with a highest absorbed dose of 0.062 or 0.127 mGy/MBq depending on the voiding schedule as described above. Absorbed doses in all other organs were at least 5-fold smaller than the bladder wall doses. **Conclusion:** With an injected activity of 370 MBq ^{18}F-FETNIM, the radiation doses are generally comparable with those of other related radionuclide imaging procedures. Specifically, in comparison with ^{18}F-fluoromisonidazole, the absorbed doses of ^{18}F-FETNIM are equal. However, special attention should be given to adequate hydration and voiding to limit the relatively high exposure of the critical organ, bladder wall, to ^{18}F-FETNIM.

Key Words: ^{18}F-fluoroerythronitromidazole; radiation dose; PET

J Nucl Med 2002; 43:1674–1680

Varying amounts of hypoxic cells exist in almost all solid tumors. These cells are known to be relatively resistant to various forms of cancer therapy (*1*). The clinical challenge is to detect the proportion of hypoxia accurately and feasibly to administer treatment specifically targeting poorly oxygenated cells (*2*,*3*). ^{18}F-Fluoroerythronitroimidazole (^{18}F-FETNIM) is a new promising tracer for imaging hypoxia in vivo using PET (*4*). ^{18}F-FETNIM is a 2-nitroimidazole compound structurally related to ^{18}F-fluoromisonidazole (^{18}F-FMISO), a more widely used tracer for detection of hypoxia (*5*,*6*). Reduced nitroimidazole metabolites make covalent bonds in low oxygen concentration and are therefore accumulated into viable hypoxic cells (*4*). ^{18}F-FETNIM is more hydrophilic than ^{18}F-FMISO and thus can be expected to be eliminated more rapidly from well-oxygenated tissues, allowing a higher tumor-to-background ratio than the more lipophilic tracers (*4*).

We are currently studying the applicability of ^{18}F-FETNIM PET to measure tumor hypoxia in human head and neck cancer (*7*,*8*). For accurate radiation dosimetry of ^{18}F-FETNIM PET, the critical organs and effective dose should be defined in humans. Indeed, effective dose as a means of characterizing the biologic significance of radiation exposure is used as a reference when evaluating the benefits and risks associated with ^{18}F-FETNIM. Specifically, the dosimetry of ^{18}F-FETNIM should be compared with that of ^{18}F-FMISO, which has been available for imaging hypoxia for more than a decade. The radiation dose in ^{18}F-FMISO PET has been found to be comparable with other widely used clinical nuclear medicine procedures, and the critical organ was the bladder wall (*9*).

The MIRD schema developed by the MIRD Committee of the Society of Nuclear Medicine is a common procedure for radiation dose calculations in nuclear medicine (*10*). The equation to the mean absorbed dose (D) in a target organ (r_k), from injected dose (A_0) is:

$$\frac{\bar{D}(r_k)}{A_0} = \sum_h \tau_h S(r_k \leftarrow r_h),$$

where the S value contains physical aspects of the dose calculation and the residence time (τ_h) includes the kinetics of the radionuclide in the source organ (h). Although physical factors of ^{18}F decay are well documented, the task for the dosimetrist is to measure the residence time or the cumulated activity in the source organ.

We describe a procedure to measure residence times within various body tissue compartments using quantitative PET measurements from patients with cancer. Because ^{18}F-FETNIM has been found to be more hydrophilic than ^{18}F-FMISO, with octanol-to-water coefficients of 0.17 and 0.4 (*4*), respectively, it is crucially important to accurately es-

Received Feb. 8, 2002; revision accepted Jul. 25, 2002.

For correspondence or reprints contact: Tuula Tolvanen, MSc, Turku PET Centre, Turku University Central Hospital, P.O. Box 52, 20521 Turku, Finland.
E-mail: tuula.tolvanen@tyks.fi

timate the bladder wall radiation dose. ^{18}F-FETNIM is mainly excreted via the urinary tract and we estimated cumulated activity in the urinary bladder from measured urine samples.

MATERIALS AND METHODS

Patients

Measurements from 27 patients (21 men, 6 women) who underwent ^{18}F-FETNIM PET scanning between November 1999 and May 2001 were used for the dosimetry study. All patients had a histologically verified cancer. Six male oncologic patients were scanned for thorax or abdomen to acquire data from the heart, lung, liver, kidney, spleen, pancreas, red bone marrow, muscle, and intestine tissues. Dynamic data from neck muscle (n = 14) and brain tissue (n = 3) were obtained from head and neck cancer patients who were enrolled in the study evaluating tumor hypoxia (*7*). Normal tissues used for dosimetry were distant from the site of the tumor and the distribution of ^{18}F-FETNIM in the whole body was assumed to be undisturbed by the hypoxia-specific uptake. Urine samples were collected from 27 patients to calculate the activity excreted in urine. Patients were advised to fast at least 4 h before the study.

The study protocol was approved by the joint ethical committee of Turku University and Turku University Central Hospital and permission to use ^{18}F-FETNIM in patient studies was granted by the Finnish National Agency for Medicines. All patients signed informed consent before entering the study.

Dynamic PET Studies

PET studies were performed with an Advance PET scanner (General Electric Medical Systems, Milwaukee, WI) operated in 2-dimensional mode. The scanner consists of 18 rings of bismuth germinate detectors, yielding 35 transverse slices spaced by 4.25 mm. The imaging field of view (FOV) is 15.2 cm in axial length and 55 cm in diameter (*11*).

Scatter correction, random counts, and dead-time corrections were all incorporated into the reconstruction algorithm. Attenuation factors were measured with 2 rotating rod sources containing ^{68}Ge/^{68}Ga for each subject before injection, and images were corrected for radiation attenuation. The central 55-cm FOV was used in thorax and abdomen image reconstruction, whereas the FOV in head and neck studies was 30 cm, resulting in an image pixel size of 4.29 × 4.29 mm and 2.34 × 2.34 mm in a 128 × 128 image matrix, respectively. A transaxial Hanning filter with a cutoff frequency of 4.6 mm was used.

^{18}F-FETNIM was synthesized from 1-(2′-nitro-1′-imidazolyl)-2,3-*O*-isopropylidene-4-tosyloxybutane by nucleophilic displacement of the tosyloxy group with ^{18}F-F$^-$. The radiochemical synthesis of ^{18}F-FETNIM is described in detail elsewhere (*4,8*). The radiochemical purity of ^{18}F-FETNIM exceeded 95% and the specific radioactivity exceeded 300 GBq/μmol.

Before imaging, patients had venous lines inserted in the antecubital forearm for tracer injection. On the opposite arm, the radial artery was cannulated in 20 patients for continuous blood sampling during PET acquisition. All PET studies started with a 10-min transmission scan. The tracer was injected as a 15-s intravenous bolus (median dose, 366 MBq; range, 288–385 MBq). The 3 different imaging protocols used in this study all started as dynamic scans immediately after injection and they are illustrated in Figure 1. The first part of the acquisition took 20, 60, or 120 min, and additional later imaging sequences were performed between 80 and 120 min, 160 and 180 min, or 210 and 240 min, respectively. The frame rates were as follows: protocol 1 (1 dynamic part), 8 × 15 s, 28 × 60 s, and 6 × 300 s; protocol 2 (2 dynamic parts), 4 × 30 s, 3 × 60 s, 5 × 180 s, 8 × 300 s, and 6 × 600 s; the second part, between 160 and 180 min, 3 × 400 s; protocol 3 (3 dynamic parts), 4 × 30 s, 3 × 60 s, 5 × 180 s; the second part, between 80 and 120 min, 4 × 600 s; the third part, between 210 and 240 min, 3 × 600 s. Totally, every patient was imaged for at least 60 min. The patients were allowed to stand up and relax between scanning sessions in protocols 2 and 3.

Measurements of ^{18}F Activity in Urine and Blood Samples

Patients were asked to void immediately before ^{18}F-FETNIM injection. After completion of the PET scanning, the total activity in the whole urine volume was determined within 27−250 min after administration. Urinary samples of 2.5 mL were measured with the dose calibrator (VDC404; Veenstra Instrumenten bv,

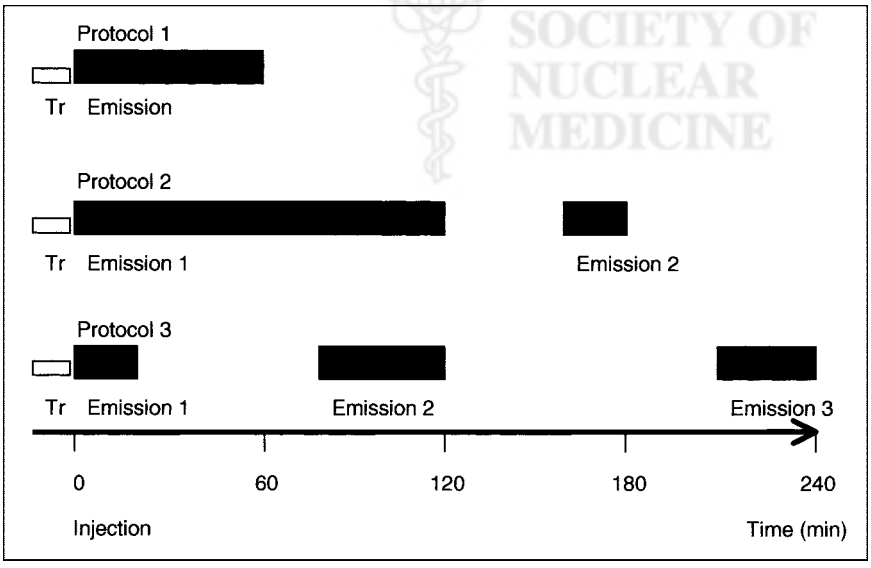

FIGURE 1. Dynamic imaging protocols used for ^{18}F-FETNIM PET dosimetric study. Protocol 1 was used specifically to measure source organ uptake in thorax and abdomen. Protocols 2 and 3 were used in head and neck cancer patients. Frame rates varied in 3 protocols and are explained in text. Tr = transmission scan.

Joure, The Netherlands). The fraction of injected dose excreted into urine was calculated for 27 patients.

During the imaging session about 20 sequential blood samples were collected. In the beginning of the study samples were taken frequently to detect the peak of the plasma activity curve. The activity was measured with an automatic γ-counter (Wizard; Wallac-EG&G, Turku, Finland) cross-calibrated with the PET scanner via the dose calibrator. Twenty arterial plasma curves were obtained in this fashion.

Residence Times in Source Regions

The source organ residence times were determined from quantitative PET images with a 4-step procedure. First, the time course of activity concentration was measured from dynamic PET images. Regions of interest (ROIs) were manually defined on source organs in 3 or 4 contiguous planes in each patient. The outline of the source organs was readily visible on the summed ^{18}F-FETNIM PET images in most cases. The first 2 min were summed to indicate vascular activity in the spleen, lungs, and heart. The last 25 min were summed for detection of retention in the source organs. The ROI for red bone marrow was defined to transmission images because of the absence of any detectable uptake of ^{18}F-FETNIM in vertebral bodies. The compatibility of transmission and emission images was ensured with anatomic landmarks. The average of values in adjacent planes was assumed to represent the activity concentration of ^{18}F-FETNIM and its metabolites in the whole organ. Second, time–activity curves of the patients were normalized to a 70-kg reference adult weight and 1-MBq injection as follows:

$$C'(t) = C(t)\left(\frac{1}{A_0}\right)\left(\frac{W}{\overline{W}}\right),$$

where $C'(t)$ is the normalized activity concentration (kBq/mL), $C(t)$ is the measured activity concentration from ROI analysis, A_0 is the injected activity (MBq), W is the patient weight (kg), and $\overline{W}$ is 70 kg, respectively. Third, normalized but not decay-corrected activity concentration data of all patients for each tissue (including blood) were plotted against time and averaged in each frame. Fourth, the time course of activity after the last measured frame was assumed to continue in compliance with the physical half-life of ^{18}F. The cumulated activity concentration was measured as area under the time–activity curve. The total activity was obtained by multiplying the cumulated activity per milliliter with organ volumes derived from a 70-kg reference man (*12*). Heart contents were considered to be 150 mL of blood, and the remainder of the blood was considered to contribute to the remainder of the body residence time (*13*).

The physical decay was removed from the arterial plasma curve, and the area under the normalized curve was integrated to represent the ^{18}F-FETNIM residence time in blood. The concentration of ^{18}F-FETNIM or its metabolites in plasma and blood was assumed to be comparable. This was verified by comparing plasma and blood activities in 6 patients. The heart content residence time measured with the ROI technique as described above was comparable to the residence time measured from the arterial plasma curve.

The cumulative activity in the urinary bladder was estimated from combined patient data. The percentage of injected dose in voided urine in all patients was combined into 1 dataset. The empiric formula of exponential in-growth, $A_B(1 - e^{-bt})$, was used to fit the activity in urinary bladder measurements as follows (*9*): The rate coefficient for clearance, b, was estimated by adjusting the total excretion fraction of the injected dose in urine, A_B, to different values between 40% and 100% to fit the measured data. Physical decay was removed from fitted curves and the data were normalized to injection of 1 MBq of tracer. The area under the curve represents the cumulated activity in the bladder from injection of 1 MBq. A 2- or 4-h integration time and the average of the measured volume (351 mL) were used for calculation of the residence time of the urinary bladder content.

Cumulated activity in the remainder of the body was calculated as follows:

$$\bar{A}_{RB} = A_0 \int_0^T e^{-\ln 2/T_{1/2}\, t} dt + A_T \int_T^\infty e^{-\ln 2/T_{1/2}\, t} dt - \sum_i A_i,$$

where A_{RB} is the cumulated activity in the remainder of the body, A_0 is the injected dose, A_T is the injected dose minus the excreted activity at time T = 2 h or T = 4 h, and A_i is the cumulated activity in the measured source organ.

The residence time is the quotient of the cumulated activity for any source organ and the total activity injected to the patient.

Radiation Dose Calculations

Absorbed doses were calculated according to Publication 60 (*14*) procedures of the International Commission of Radiation Protection (ICRP) with MIRDOSE3 software (*15*) (Oak Ridge Associated Universities, Oak Ridge, TN). MIRDOSE software calculates S values to selected radionuclide and anthropomorphic phantom. Aspects embodied in the S value are the physical characteristics of ^{18}F (half-life, emission types and energies, decay products, and penetration ability of the radiation) and the fraction of absorbed energy to each target organ from each source region in the body. Measured residence times in the brain, stomach, upper large intestine, heart content, kidneys, lungs, muscle, pancreas, red marrow, spleen, urinary bladder, and the remainder of the body were given as an input. The residence times for each source region were calculated as an integral of the normalized time–activity curve from 0 to infinity, except in urinary bladder content where voiding time was considered. The conservative method of estimating the clearance half-time with physical half-life (109.8 min) instead of the effective clearance half-time after the last measured time point was used.

RESULTS

The main radiation source regions in ^{18}F-FETNIM distribution were urinary bladder content, kidney, liver, spleen, blood, and muscle. On PET images, these regions were visually found to contain more activity than the rest of the body. The brain was included in the source organs because clearance curves were analyzed for clinical use and information on the penetration of ^{18}F-FETNIM across the blood–brain barrier was considered important. The stomach, pancreas, and upper large intestine were sometimes detectable, and for those patients these organs were accepted for dosimetry evaluation. Spatial location was ensured with coreading of corresponding CT images. We gave specific attention to the dose of red marrow, being aware of its

sensitivity to radiation even though bony structures were not directly visualized on ^{18}F-FETNIM PET images. The time–activity curves for the source organs are shown in Figures 2 and 3. Patient-to-patient variation in time–activity curves for the kidneys can be seen because of differences in normal renal function.

Urinary excretion of ^{18}F-FETNIM was in the range of 6%–50% of injected activity within 250 min after injection. Figure 4 illustrates the fitting from the entire set ($n = 27$) of voided activity fractions. The graph suggests that up to 60% of ^{18}F-FETNIM is cleared through the urinary pathway, which can be also seen from the distribution fraction.

The residence times of ^{18}F-FETNIM in the 13 source regions are given in Table 1. The radiation dose estimates for an adult weighing 70 kg are given in Table 2. The highest absorbed doses were found for the urinary bladder wall, with 0.062 mGy/MBq or 0.127 mGy/MBq corresponding to the 2- or 4-h voiding schedule, respectively. The effective dose was estimated to be 0.015 mSv/MBq or 0.019 mSv/MBq, leading up to a 5.55-mSv or 7.03-mSv dose for the 370-MBq ^{18}F-FETNIM injection depending on the voiding protocol.

DISCUSSION

The existence of viable hypoxic cells in solid tumors and the radioresistance of those cells were recognized several decades ago. Considerable effort has been made to overcome the hypoxic radioresistance but one of the key issues is to recognize the magnitude of the problem in individual cases. Most existing methods to assess tumor oxygenation require tissue sampling or use of special probes but, lately, noninvasive methods to detect hypoxia with radionuclides and PET or SPECT have been in the focus of interest (*3*,*16*).

We have recently started to study a newly introduced nitroimidazole compound, ^{18}F-FETNIM, first synthesized by Yang et al. (*4*) for this particular application. Our initial experience in head and neck cancer indicates that some tumors show higher late ^{18}F-FETNIM uptake compared with that of adjacent neck muscles and oral mucosa (*7*), and further validation of hypoxia-specific retention of the tracer is in progress.

Clinically, tumor hypoxia has been evaluated with PET most extensively using another nitroimidazole compound, ^{18}F-FMISO (*5*,*6*). The radiation dosimetry of FMISO has been studied previously (*9*). Both organ doses and effective

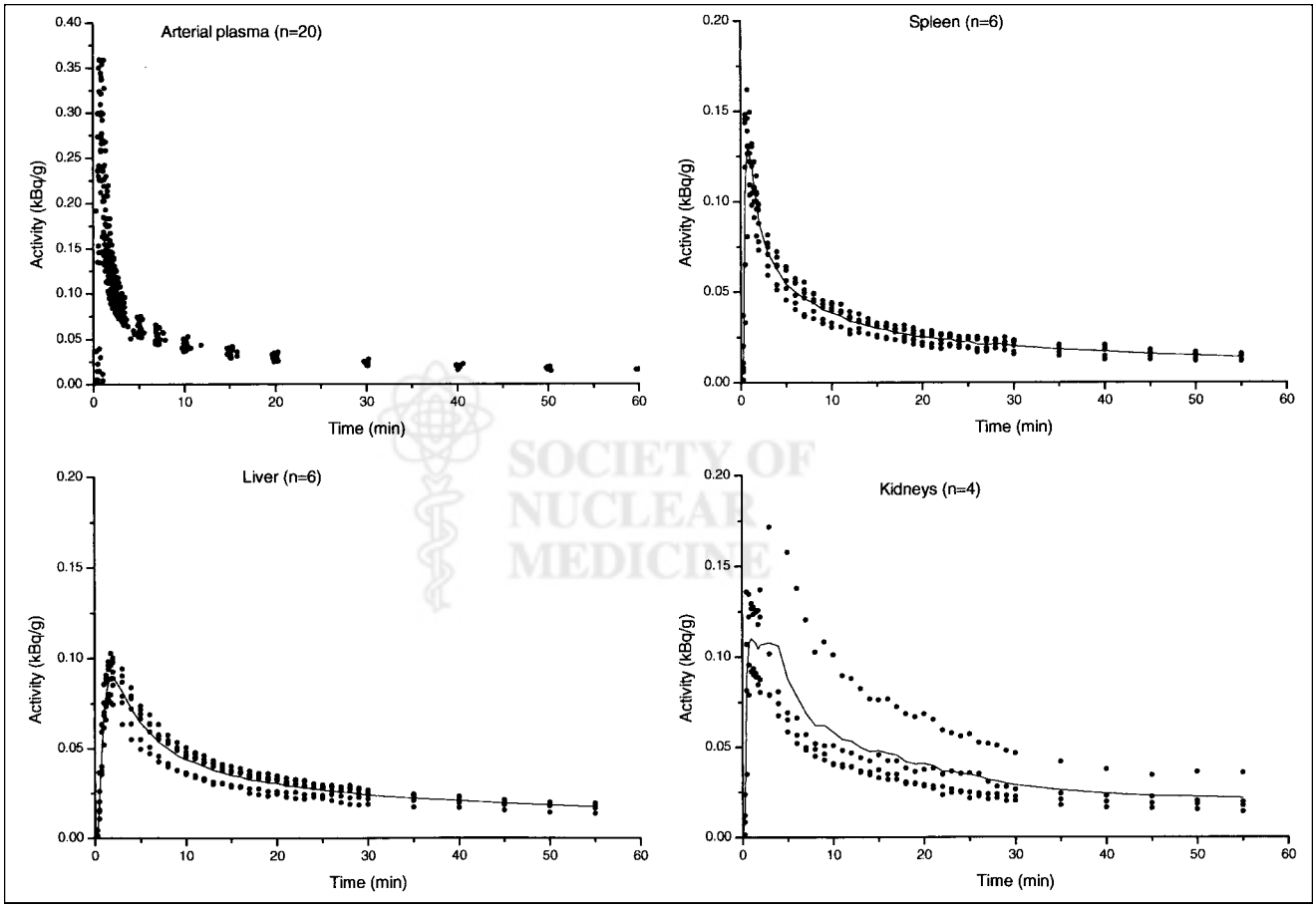

FIGURE 2. Activity of ^{18}F-FETNIM in 4 source organs shows clearly higher activity than rest of body: blood, spleen, liver, and kidneys. Solid line is mean curve of individual values. Activity has been normalized to 1-MBq injected dose and 70-kg body weight. Similar shape in curves for blood, liver, and spleen indicates that blood activity has major impact on dose of 2 parenchymal organs.

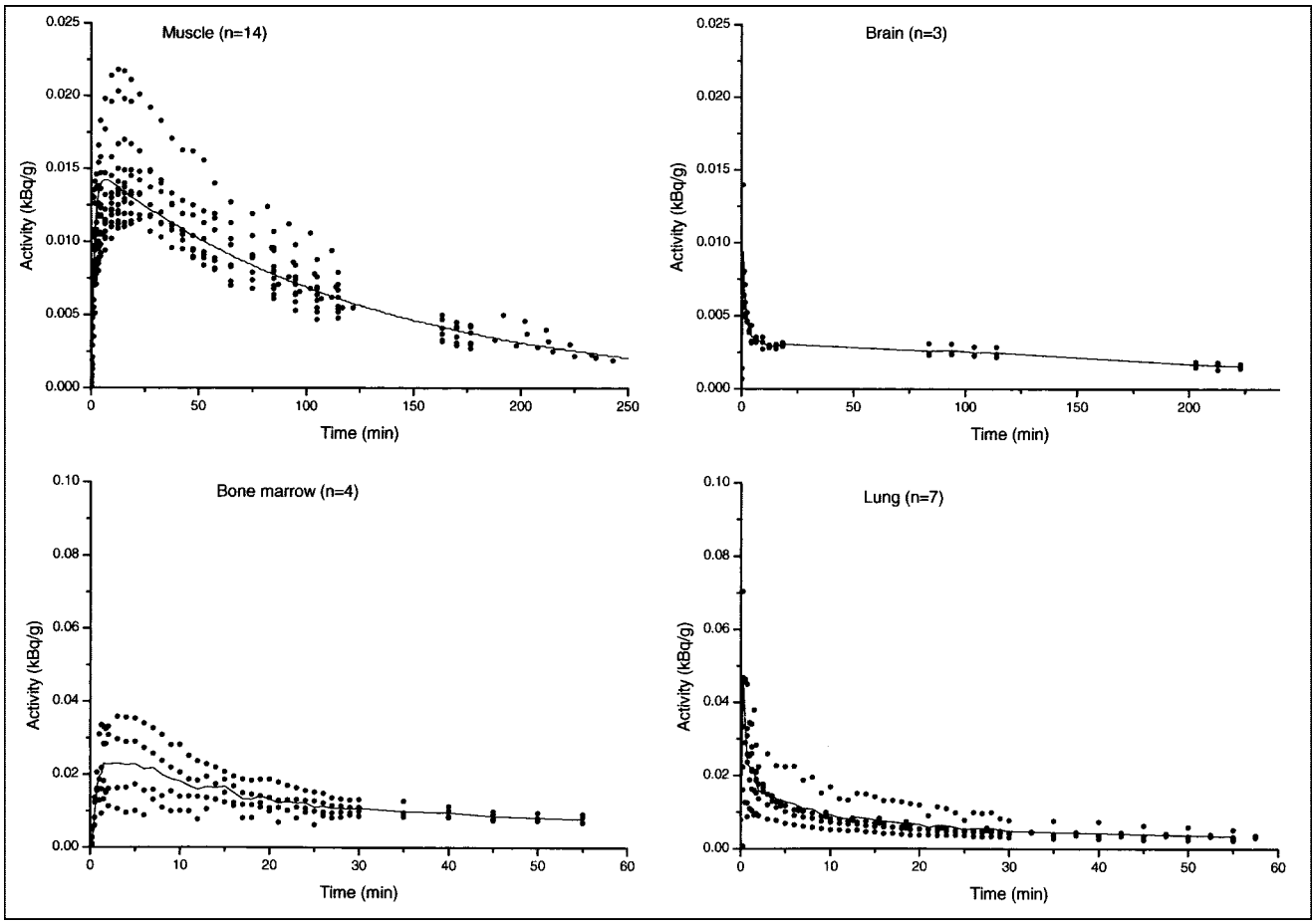

FIGURE 3. Activity of ^{18}F-FETNIM in source organs shows relatively low activity: muscle, brain, bone marrow, and lung. Solid line is mean curve of individual values. Activity has been normalized to 1-MBq injected dose and 70-kg body weight.

dose were found to be comparable with those of other commonly performed nuclear medicine tests and therefore the risks of the study were assumed to be within accepted limits. ^{18}F-FETNIM is likewise a 2-nitroimidazole and is structurally related to ^{18}F-FMISO, but, because of its greater hydrophilicity, differences are expected in absorbed doses in the urinary tract where it is predominantly excreted. Because of this it is mandatory to study the dosimetry of

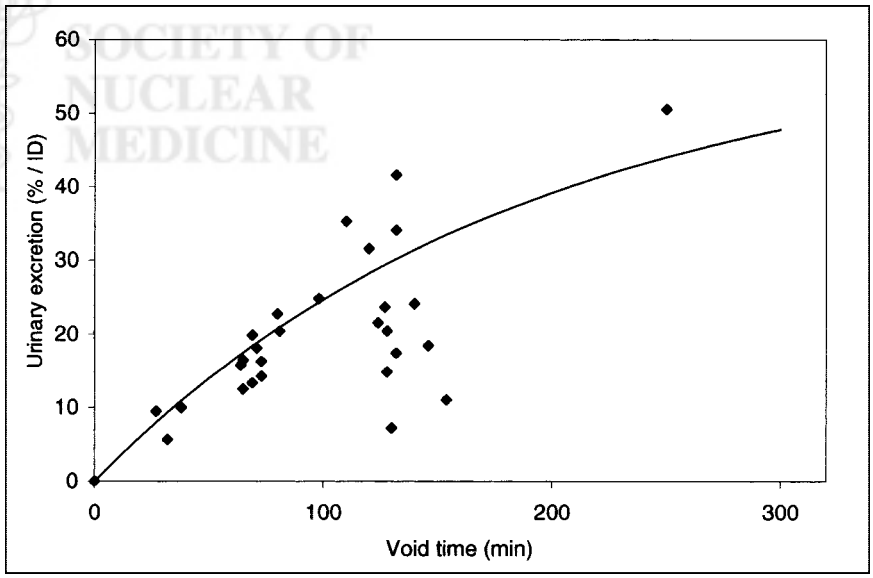

FIGURE 4. ^{18}F-FETNIM urine activity. Fitted curve is based on 28 samples from 27 patients. Note high percentage of total injected activity excreted in bladder for subjects holding urine. ID = injected dose.

TABLE 1
Residence Times of ^{18}F-FETNIM

Source organ	Time (h)	No. of patients
Brain	0.023	3
Stomach	0.009	2
Upper large intestine	0.012	3
Heart contents	0.011	20
Kidneys	0.033	4
Liver	0.152	6
Lungs	0.015	7
Muscle	1.060	6
Pancreas	0.006	2
Red marrow	0.053	4
Spleen	0.013	6
Urinary bladder content 2 h	0.110	27
Urinary bladder content 4 h	0.244	27
Rest of body 2 h	0.795	
Rest of body 4 h	0.760	

^{18}F-FETNIM in detail using the same formalism as Graham et al. (*9*). We found the effective dose of ^{18}F-FETNIM to be slightly higher than that of ^{18}F-FMISO (0.017 vs. 0.013 mSv/MBq, respectively).

Graham et al. (*9*) used the concept of "the effective dose equivalent" H_E, which is the effective dose E with different tissue-weighting factors. To facilitate comparison between ^{18}F-FMISO and ^{18}F-FETNIM radiation doses, we have calculated effective doses using both methods. The differences in radiation dosimetry terminology concerning the effective dose, the effective dose equivalent, and the total body dose are described elsewhere (*17,18*). The differences in absorbed doses in Table 2 between ^{18}F-FMISO and ^{18}F-FETNIM are consistent with the different octanol-to-water partition coefficients measured for the 2 tracers. However, as expected, the dose to the urinary bladder wall was clearly higher for ^{18}F-FETNIM compared with that of ^{18}F-FMISO, 0.062 mGy/MBq versus 0.021 mGy/MBq, respectively. This implies that adequate hydration of the patient is essential in ^{18}F-FETNIM PET studies to dilute the activity in the bladder, and attention should be given to the voiding schedule both before and after injection. The urinary bladder wall dose from positron emission radiation can be reduced by increasing the initial bladder content volume as much as possible at the time of injection (*19*). The first voiding time

TABLE 2
Absorbed Doses of ^{18}F-FETNIM to Target Organs

	Voiding interval		^{18}F-FMISO*	^{18}F-FDG	
Target organ	2 h (mGy/MBq)	4 h (mGy/MBq)	2 h (mGy/MBq)	ICRP 60† (mGy/MBq)	MIRD 19‡ (mGy/MBq)
Adrenals	0.012	0.012	0.017	0.012	
Brain	0.006	0.006	0.009	0.028	0.046
Breasts	0.007	0.007	0.012	0.009	
Gallbladder wall	0.014	0.014	0.015	0.012	
Lower large intestine wall	0.012	0.014	0.014	0.015	
Small intestine	0.012	0.012	0.011	0.013	
Stomach	0.012	0.012	0.013	0.011	
Upper large intestine wall	0.014	0.015	0.014	0.012	
Heart wall	0.011	0.011	0.019	0.062	0.068
Kidneys	0.027	0.027	0.016	0.021	0.021
Liver	0.024	0.024	0.018	0.011	0.024
Lungs	0.008	0.008	0.010	0.010	0.015
Muscle	0.012	0.012	0.014	0.011	
Ovaries	0.013	0.014	0.018	0.015	0.011
Pancreas	0.019	0.019	0.017	0.012	0.014
Red marrow	0.012	0.012	0.010	0.011	0.011
Bone surfaces	0.011	0.011	0.008	0.011	
Skin	0.007	0.007	0.005	0.008	
Spleen	0.020	0.020	0.016	0.011	0.015
Testes	0.010	0.011	0.015	0.012	0.011
Thymus	0.009	0.009	0.016	0.011	
Thyroid	0.009	0.009	0.015	0.010	
Urinary bladder wall	0.062	0.127	0.021	0.160	0.073
Uterus	0.015	0.018	0.018	0.021	0.012
Total body	0.011	0.011	0.013		
Effective dose equivalent§	0.017	0.021	0.013		
Effective dose§	0.015	0.019		0.019	

*Median values from ^{18}F-FMISO dosimetry study (*9*).
†Median values from ^{18}F-FDG ICRP dosimetry (*14*).
‡Median values from ^{18}F-FDG MIRD 19 dosimetry (*20*).
§Units are mSv/MBq.

should be optimized on the basis of excretion rate of ^{18}F-FETNIM and currently we recommend that it should not be delayed beyond 120 min. Normal variation in renal function affects absorbed doses to the kidneys significantly. If renal function is suboptimal, bladder catheterization should be considered.

Besides the two 2-nitroimidazole compounds, Table 2 also shows dosimetry for the most commonly used ^{18}F-labeled tracer, ^{18}F-FDG (*19*,*20*), and indicates that only minor differences can be demonstrated in target organ doses between the 3 tracers. ^{18}F-FDG shows high activity in the brain, heart, and bladder and low activity in the liver and pancreas in comparison with both ^{18}F-FMISO and ^{18}F-FETNIM. The high bladder activity of both ^{18}F-FDG and ^{18}F-FETNIM may be comparable because of the differences in the method of measurement between this study and that published by ICRP (*14*).

For calculation of the residence time, the activity concentration of this PET study is converted into the activity accumulation of the organ, assuming the tissue density of 1 g/mL. In the calculation of organ doses and effective dose in Table 2, the 70-kg adult phantom with both male and female genitals was used.

CONCLUSION

The effective dose of ^{18}F-FETNIM PET is well within the range of several related nuclear medicine procedures such as ^{18}F-FDG PET and ^{18}F-FMISO PET. With the exception of the urinary tract, the measured absorbed doses are similar to reported doses for ^{18}F-FMISO, the most commonly used tracer to image hypoxia with PET. Up to 60% of the compound is excreted through the kidneys, and the critical organ is, therefore, the bladder wall. The radiation dose to the bladder can best be controlled by increasing the urine excretion rate with frequent bladder voiding after injection.

ACKNOWLEDGMENTS

The authors thank the medical laboratory technologists and radiographers of the Turku PET Centre for their skillful assistance and cooperation. Financial support was provided in part by the Finnish Cancer Foundation, the Southwestern Finnish Cancer Foundation, and the Turku University Foundation.

REFERENCES

1. Hall EJ. Radiosensitizers and bioreductive drugs. In: Hall EJ, ed. *Radiobiology for the Radiologist.* Philadelphia, PA: J.B. Lippincott; 1994:165–181.
2. Brown JM. Exploiting the hypoxic cancer cell: mechanisms and therapeutic strategies. *Mol Med Today.* 2000;61:57–162.
3. Chapman JD, Engelhardt EL, Stobbe CC, Schneider RF, Hanks GE. Measuring hypoxia and predicting tumor radioresistance with nuclear medicine assays. *Radiother Oncol.* 1998;46:229–237.
4. Yang DJ, Wallace S, Cherif A, et al. Development of F-18-labeled fluoroerythronitroimidazole as a PET agent for imaging tumor hypoxia. *Radiology.* 1995; 194:795–800.
5. Rasey JS, Koh WJ, Grierson JR, Grunbaum Z, Krohn KA. Radiolabelled fluoromisonidazole as an imaging agent for tumor hypoxia. *Int J Radiat Oncol Biol Phys.* 1989;17:985–991.
6. Koh WJ, Rasey JS, Evans ML, et al. Imaging of hypoxia in human tumors with [F-18]fluoromisonidazole. *Int J Radiat Oncol Biol Phys.* 1992;22:199–212.
7. Lehtiö K, Oikonen V, Grönroos T, et al. Imaging of blood flow and hypoxia in head and neck cancer: initial evaluation with [^{15}O]H_2O and [^{18}F]fluoroerythronitroimidazole PET. *J Nucl Med.* 2001;42:1643–1652.
8. Grönroos T, Eskola O, Lehtiö K, et al. Pharmacokinetics of [^{18}F]FETNIM: a potential marker for PET. *J Nucl Med.* 2001;42:1397–1404.
9. Graham MM, Peterson LM, Link JM, et al. Fluorine-18- fluoromisonidazole radiation dosimetry in imaging studies. *J Nucl Med.* 1997;38:1631–1636.
10. Howell RW, Wessels BW, Loevinger R, in collaboration with the MIRD Committee. The MIRD perspective 1999. *J Nucl Med.* 1999;40(suppl):3S–10S.
11. DeGrado TR, Turkington TG, Williams JJ, Stearns CW, Hoffman JM, Coleman RE. Performance characteristics of a whole-body PET scanner. *J Nucl Med.* 1994;35:1398–1406.
12. Snyder WS, Cook MJ, Nasset ES, Karhausen LR, Howells GP, Tipton IH. *Report of the Task Group on Reference Man.* Oxford, U.K.: Pergamon Press; 1974:325–327.
13. Deterding TA, Votaw JR, Wang CK, et al. Biodistribution and radiation dosimetry of the dopamine transporter ligand. *J Nucl Med.* 2001;42:376–381.
14. International Commission on Radiological Protection. *1990 Recommendation of the International Commission on Radiological Protection.* Publication 60. Oxford, U.K.: Pergamon Press; 1990:4–11.
15. Stabin MG. MIRDOSE: personal computer software for internal dose assessment in nuclear medicine. *J Nucl Med.* 1996;37:538–546.
16. Chapman JD, Zanzonico P, Ling CC. On measuring hypoxia in individual tumors with radiolabeled agents. *J Nucl Med.* 2001;42:1653–1655.
17. Stabin MG, Stubbs JB, Watson EE. Dosimetry of swallowed non-absorbed technetium 99m radiopharmaceuticals in paediatric patients. *Eur J Nucl Med.* 1991;18:288–292.
18. Johansson L, Mattsson S, Nosslin B, Leide-Svegborn S. Effective dose from radiopharmaceuticals. *Eur J Nucl Med.* 1992;19:933–938.
19. Dowd MT, Chen CT, Wendel MJ, Faulhaber PJ, Cooper MD. Radiation dose to the bladder wall from 2-[^{18}F]fluoro-2-deoxy-D-glucose in adult humans. *J Nucl Med.* 1991;32:707–712.
20. Hays MT, Watson EE, Thomas SR, Stabin M. MIRD dose estimate report no. 19: radiation absorbed dose estimates from ^{18}F-FDG. *J Nucl Med.* 2002;43:210–214.